# X-ray absorption at the L 2 , 3 edge of an anisotropic single crystal: Cadmium (0001)

P. Le Fèvre, H. Magnan, D. Chandesris

# X-ray absorption at the $L_{2,3}$ edge of an anisotropic single crystal: Cadmium (0001)

P. Le Fèvre
*Laboratoire pour l'Utilisation du Rayonnement Electromagnetique (LURE), Université Paris Sud, 91405 Orsay Cedex France and Service de Recherche sur les Surfaces et l'Irradiation de la Matiere, Commissariate a'l'Energie Atomique Saclay, 91191 Gif sur Yvette, France*

H. Magnan
*Laboratoire pour l'Utilisation du Rayonnement Electromagnetique (LURE), Université Paris Sud, 91405 Orsay Cedex France and Service de Recherche sur les Surfaces et l'Irradiation de la Matiere, Commissariate a'l'Energie Atomique Saclay, 91191 Gif sur Yvette, France*

D. Chandesris
*Laboratoire pour l'Utilisation du Rayonnement Electromagnetique (LURE), Université Paris Sud, 91405 Orsay Cedex France*
(Received 15 January 1996)

Surface extended x-ray-absorption fine structure (EXAFS) is a very powerful technique for the crystallographic characterization of adsorbed atoms, layers, and thin films. The linear polarization of the synchrotron radiation is used to infer direct information about the crystallographic anisotropy of these systems. For the $K$ absorption edge, the polarization dependence of the EXAFS signal is simple: the contribution of each bond is weighted by a factor $\cos^2\theta$, where $\theta$ is the angle between the direction of the bond and the linear polarization of the x rays. For $L_{2,3}$ absorption edges, the polarization dependence is more complicated, since the initial $p$ state can be excited to a final state of $s$ or $d$ symmetry. The angular dependences of these two terms are strongly different. We show here, with a study on a bulk anisotropic system, cadmium, that the two terms have to be considered and that neglecting the $p$ to $s$ transitions in the analysis of angular-dependent spectra leads to errors in bond-length determination as high as 0.1 Å. [S0163-1829(96)01928-5]

## I. INTRODUCTION

Up to now, most of the surface extended x-ray-absorption fine structure (EXAFS) studies have been performed measuring x-ray-absorption spectra at the $K$ edge of the adsorbed element.[1–4] In this case, the initial state of the photoelectron is a $1s$ state and the photoabsorption probability involves only states of $p$ symmetry in the electric dipole approximation. It has been shown,[5] in the single scattering approximation, that the contribution of each neighbor is then weighted by a factor $\cos^2\theta$, where $\theta$ is the angle between the polarization of the x rays and the neighbor direction. At $L_2$ or $L_3$ edges, in the electric dipole approximation, the $2p$ initial state is excited to final states of both $s$ and $d$ symmetry, leading to a $s$-$d$ crossed term that is nonzero for anisotropic absorbers.[6,7] The interpretation of the angular dependence of the XAFS spectrum is then more complicated: the $s$ states give no orientational dependence but $d$ states can have a complex angular dependence. Then, quantitative analysis of anisotropic systems studied with polarized light will strongly depend on the relative weights of the different transition probabilities. In this paper, the term ''anisotropic'' refers to systems where the absorption cross section due to the dipole transition is not isotropic: noncubic single crystals, thin films or adsorbates. On the contrary, for single crystals with a cubic structure, powders, polycrystals, or amorphous solids, the absorption cross section is isotropic.[8]

The theoretical expression of the the EXAFS modulation function, $\chi(k)$, in the single scattering approximation, at the $L_{2,3}$ edges has been established by Heald and Stern.[6] Defining $M_{01}$ and $M_{21}$ as the radial dipole matrix elements between the $2p$ $(l=1)$ atomic wave function and the $d$ $(l=2)$ and $s$ $(l=0)$ final states, the EXAFS formula is[6,7,9] in the plane wave approximation:

$$\chi(k)=\sum_i \frac{B_i(k)}{kR_i^2}\frac{\exp^{-2k^2\sigma_i^2}\exp^{-[2R_i/\lambda(k)]}}{|M_{21}|^2+\frac{1}{2}|M_{01}|^2}\times[\chi_1(k)+\chi_2(k)+\chi_3(k)] \quad (1)$$

with

$$\chi_1(k)=\sum_{j=1}^{N_i}\tfrac{1}{2}(1+3\cos^2\theta_j^i)|M_{21}|^2\sin[2kR_i+\varphi_1(k)],$$

$$\chi_2(k)=\sum_{j=1}^{N_i}(1-3\cos^2\theta_j^i)M_{01}M_{21}\sin[2kR_i+\varphi_2(k)],$$

$$\chi_3(k)=\tfrac{1}{2}N_i|M_{01}|^2\sin[2kR_i+\varphi_3(k)],$$

where $k$ is the photoelectron wave vector, $B_i(k)$ is the backscattering amplitude from each of the $N_i$ neighboring atoms of the $i$th shell with a Debye-Waller factor of $\sigma_i$ and at a distance $R_i$ away. $\theta_j^i$ is the angle between the polarization vector and the $j$th neighbor of the $i$th shell. The term $\exp^{-[2R_i/\lambda(k)]}$ is due to inelastic losses, $\lambda$ being the mean free path of the photoelectron. The total phase functions are

$$\varphi_1(k)=2\delta_2(k)+\delta^i(k),$$

 

$$\varphi_2(k)=\delta_0(k)+\delta_2(k)+\delta^i(k),$$

$$\varphi_3(k)=2\,\delta_0(k)+\delta^i(k).$$

$\delta_0$ and $\delta_2$ are, respectively, the phase shifts due to the central atom potential for outgoing waves with $l=0$ and $l=2$ symmetries. $\delta^i$ is the backscattering phase shift.

$\chi(k)$ is the sum of three terms corresponding to the final state of pure $d$ ($\chi_1$), pure $s$ ($\chi_3$), and coupled $s$ and $d$ symmetries ($\chi_2$). For convenience we define[6,7]

$$\Delta\varphi(k)=\delta_0(k)-\delta_2(k),$$

then $\varphi_2=\varphi_1+\Delta\varphi$ and $\varphi_3=\varphi_1+2\Delta\varphi$, and

$$c=\frac{|M_{01}|}{|M_{21}|}.$$

For one shell of neighbors ($N$ identical atoms at a distance of $R$) Eq. (1) is rewritten as

$$\chi(k)=\frac{A'(k)}{kR^2}\frac{1}{1+\frac{1}{2}c^2}\sum_{j=1}^{N}\{\tfrac{1}{2}(1+3\cos^2\theta_j)\sin[2kR+\varphi_1(k)]+c(1-3\cos^2\theta_j)\sin[2kR+\varphi_1(k)+\Delta\varphi(k)]+\tfrac{1}{2}c^2\sin[2kR+\varphi_1(k)+2\Delta\varphi(k)]\},\tag{2}$$

where $A'(k)$ is the total amplitude function including Debye-Waller and mean-free-path terms.

In this EXAFS formula, the three terms do not have the same amplitude and phase functions and have different angular dependences: $\chi_1$ varies as $1+3\cos^2\theta_j$, $\chi_2$ varies as $1-3\cos^2\theta_j$, and $\chi_3$ is not angular dependent. The angular dependence of the first term is similar to a $K$-edge one but with a lower selectivity: each bond always contributes to the signal even if the polarization direction of the x rays is perpendicular to it. The third term does not depend on $\theta_j$ since it represents the $p$ to $s$ transitions. The second term, the crossed one, vanishes in isotropic crystals where $\langle\cos^2\theta_j\rangle=\frac{1}{3}$. In anisotropic systems the $\chi_2$ term cannot be neglected *a priori*. Its relative weight will depend on the value of $c$.

The ratio $c$ has been calculated[9] and is found to be approximately 0.2 for atoms of atomic number $Z>20$ and relatively independent of $k$. Then, in Eq. (2), $\chi_3$ can be neglected with respect to $\chi_1$. The goal of our study is to determine experimentally the value of $c$ and $\Delta\varphi$ and to evaluate, on a given system, the error done on coordination number and bond lengths determination when the approximation $c=0$ is done.

The first study of anisotropic systems at the $L_3$ edge has been published by Heald and Stern.[6] They have determined the value of $c$ from the angular dependence of the tungsten $L_3$ edge spectrum on $WSe_2$. The authors compare the EXAFS oscillations for two different incident angles of the X rays: 0° and 47°. The anisotropy of the structure is very weak and concerns only the number of neighbors. The estimation $c\simeq 0.2$ is made assuming $\Delta\varphi=0$. The other studies[7,10] have used this value of $c$ to determine unknown anisotropic structures and have discussed the $\Delta\varphi=0$ approximation.

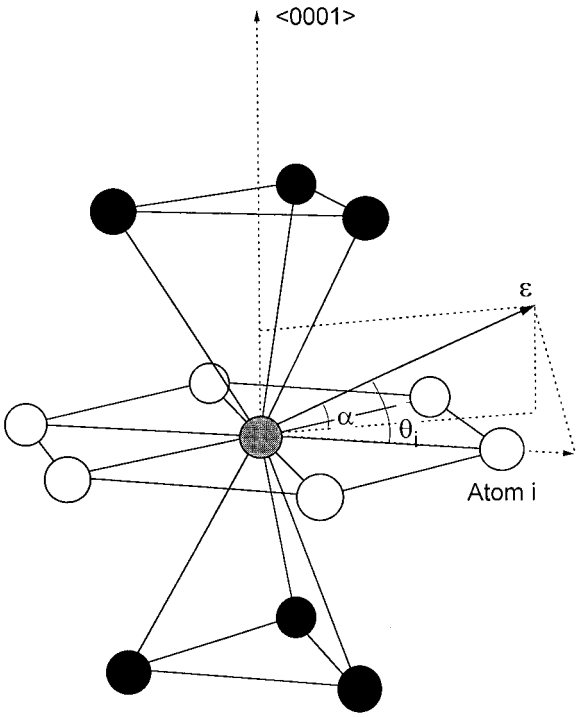


FIG. 1. First-nearest-neighbors shell of a cadmium atom. Each atom (grey) has six nearest neighbors at 2.97 Å in its (0001) plane (white atoms) and six others at 3.254 Å (black atoms). The polarization vector $\varepsilon$ of the x rays forms an angle $\theta_i$ with the $i$th bond, and an angle $\alpha$ with the (0001) planes of the Cd crystal.

In order to determine experimentally $c$ and $\Delta\varphi$ at the same time, we need an anisotropic system that has a known structure. The anisotropy should concern both bond lengths and coordination numbers. That is the reason why we have chosen a single crystal of cadmium, which has an hexagonal structure with $a=2.97$ Å and $c=5.53$ Å at 20 K (Fig. 1). Then, each Cd atom has 12 first nearest neighbors (NN's). Six NN's are located in the same hexagonal plane (in-plane NN's) at a distance $R_1=2.97$ Å , and six are located out of this hexagonal plane (out-of-plane NN's) at a distance $R_2=3.254$ Å .

## II. EXPERIMENTAL PROCEDURE

The experiments are performed at the Laboratoire pour l'Utilisation due Rayonnement Electromagnetique (LURE) on the surface EXAFS setup installed on the wiggler beam line of Dispositif de Collision dans l'Igloo storage ring, using a Si(111) double crystal monochromator. The single crystal of cadmium is polished and oriented by Lauë diffraction to obtain a (0001) free surface and then installed in the ultrahigh-vacuum chamber. The surface is cleaned by ionic bombardment, and no contamination is detected by Auger spectroscopy. The EXAFS spectra are recorded at the Cd $L_3$ edge (3538 eV) in the total yield mode. During the measurements the sample is maintained at 20 K in order to reduce the thermal disorder (the Debye temperature of cadmium is 209 K). To study the polarization dependence of the EXAFS spectra we vary the incident angle $\alpha$ of the x rays between $\alpha=0°$ (polarization of the x rays parallel to the

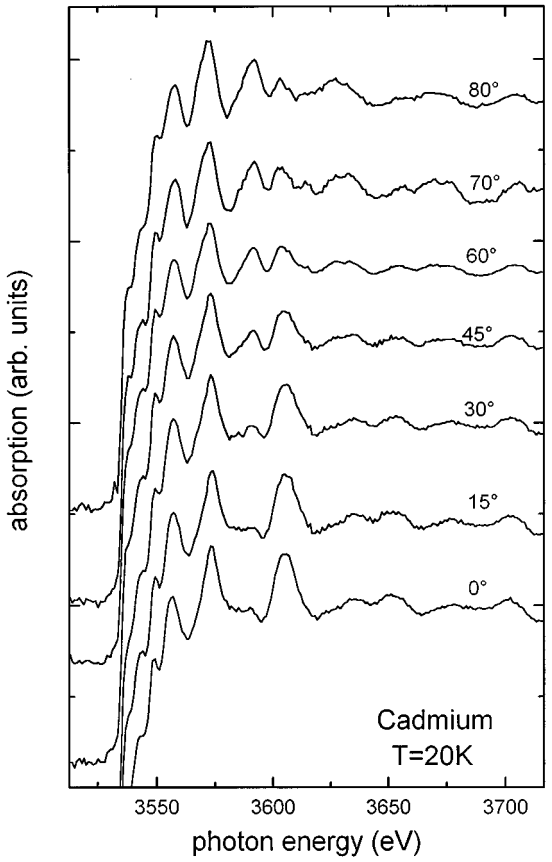


FIG. 2. X-ray-absorption raw spectra, recorded at the $L_3$ edge of Cd(0001) (3.538 eV), at 20 K, for different incident angles of the x rays.

surface) and $\alpha = 80°$ (polarization almost perpendicular to the surface). The spectra recorded with $\alpha = 0°$, 15°, 30°, 45°, 60°, 70°, and 80° are shown in Fig. 2. One can see the strong anisotropy of the spectra in particular in the energy range from 3575 to 3625 eV. We have checked that this anisotropy is not affected by the variation of the penetration depth of the x rays in the sample when the incident angle is varied: each spectrum can be reconstructed as a linear combination of two of them, using the simple formula established in the electric dipole approximation[8]

$$\chi(\alpha) = \cos^2\alpha\chi(0°) + \sin^2\alpha\chi(90°).$$

This would not be true if there were any reabsorption effect that would dump the EXAFS oscillations.

The Fourier transforms (FT's) of the spectra [$k\chi(k)$ between 1.84 Å$^{-1}$ and 6.78 Å$^{-1}$] are shown on Fig. 3. We see the shift of the first peak to higher distances when $\alpha$ is increasing. When $\alpha$ is small, the dominant term corresponds to the NN situated in the hexagonal planes at $R_1 = 2.97$ Å, and when $\alpha$ is high it corresponds to the NN out of the hexagonal planes that are at $R_2 = 3.254$ Å . Due to the small $k$ range of our data (of about 5 Å$^{-1}$), we cannot separate these two contributions. They are both mixed in the first peak of the FT. To obtain the contribution of the NN shell to the EXAFS signal, we have backtransformed this peak using the same $R$ window (between 1.96 and 3.80 Å) for all the incident angles.

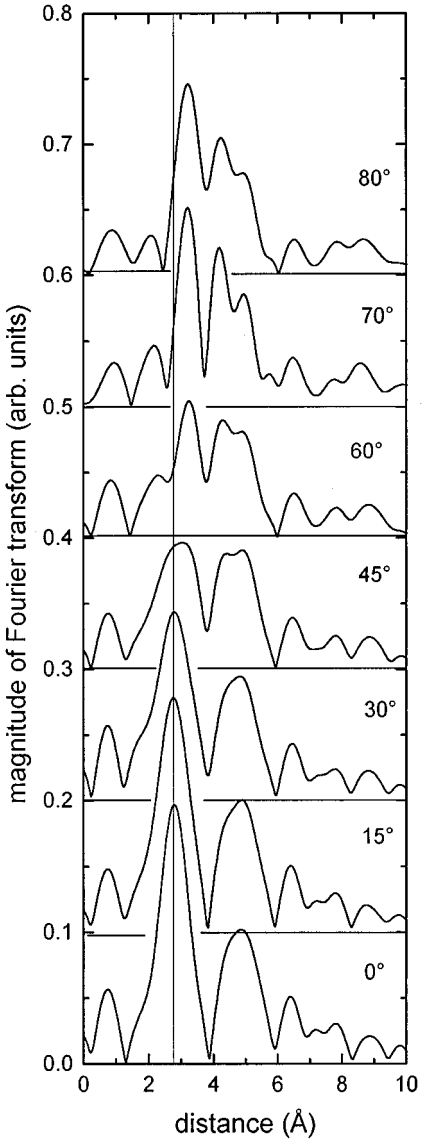


FIG. 3. Fourier transforms of $k\chi(k)$ between $k = 1.84$ and 6.78 Å$^{-1}$ for EXAFS spectra recorded at 20 K at the $L_3$ edge of Cd(0001) for different incident angles of the x rays.

### III. POLARIZATION DEPENDENCE OF THE NN SHELL

The problem now is to evaluate from these spectra the value of $c$ and $\Delta\varphi$. First, we assume that $\frac{1}{2}c^2 \ll 1$, then we can rewrite Eq. (2) at the first order in $c$ (the $\chi_3$ term disappears):

$$\chi(k,\alpha) = A'(k)\left\{ \frac{N_1^*(\alpha)}{kR_1^2}\sin[2kR_1 + \varphi_1(k)] + \frac{N_2^*(\alpha)}{kR_2^2}\sin[2kR_2 + \varphi_1(k)] + \frac{cN_1^{**}(\alpha)}{kR_1^2} \times \sin[2kR_1 + \varphi_1(k) + \Delta\varphi(k)] + \frac{cN_2^{**}(\alpha)}{kR_2^2} \times \sin[2kR_2 + \varphi_1(k) + \Delta\varphi(k)] \right\}, \quad (3)$$

TABLE I. Values of $N_1^*$, $N_2^*$, and $N_1^{**}$ (see text) for different incident angles $\alpha$ of the x rays.

| $\alpha(°)$ | 0 | 15 | 30 | MA | 45 | 60 | 70 | 80 |
|---|---|---|---|---|---|---|---|---|
| $N_1^*$ | 7.5 | 7.2 | 6.375 | 6 | 5.25 | 4.125 | 3.53 | 3.14 |
| $N_2^*$ | 4.26 | 4.61 | 5.56 | 6 | 6.87 | 8.18 | 8.87 | 9.33 |
| $N_1^{**}$ | −3 | −2.39 | −0.75 | 0 | 1.5 | 3.75 | 4.94 | 5.73 |
| $N_2^{**}$ | 3.49 | 2.78 | 0.87 | 0 | −1.74 | −4.36 | −5.74 | −6.66 |

where $N_i^*(\alpha)$ is the effective partial coordination number depending on $\alpha$ [$\alpha$ is the angle between the polarization of the x-rays incident beam and the (0001) free surface of the Cd sample]. For this Cd single crystal,

$$N_1^*(\alpha)=\sum_{j,\text{in plane}} \tfrac{1}{2}(1+3\cos^2\theta_j)=\tfrac{3}{2}(2+3\cos^2\alpha),$$

$$N_2^*(\alpha)=\sum_{j,\text{out of plane}} \tfrac{1}{2}(1+3\cos^2\theta j)$$

$$=3(4-h^2)-\tfrac{9}{2}(2-h^2)\cos^2\alpha,$$

$$N_1^{**}(\alpha)=\sum_{j,\text{in plane}} (1-3\cos^2\theta_j)=3(2-3\cos^2\alpha),$$

$$N_2^{**}(\alpha)=\sum_{j,\text{out of plane}} (1-3\cos^2\theta_j)=(h^2-2)(6-9\cos^2\alpha),$$

where $h=R_1/R_2$.

We have summarized the values of $N_i^*(\alpha)$ in Table I for each experimental incident angle. We note that $N_1^{**}(\alpha)=N_2^{**}(\alpha)=0$ for the value of $\alpha$ giving $\cos^2\alpha=\frac{2}{3}$. It is the magic angle (MA): for this value of $\alpha$ ($\alpha=35.26°$) the $\chi_2$ term vanishes as for an isotropic system and the EXAFS formula looks like the $K$-edge one.

## IV. EXPERIMENTAL DETERMINATION OF $A'(k)$ AND $\varphi_1(k)$ FROM THE MA SPECTRUM

From the magic angle experimental XAFS spectrum, it is possible to extract the amplitude $A'(k)$ and the phase function $\varphi_1$. As can be seen on Fig. 4(a), the EXAFS signal is very small for the $k$ values between 5 and 7 Å$^{-1}$. This is due to the destructive interference between the two terms created by the two NN distances, $R_1=2.97$ and $R_2=3.254$ Å, which gives a beating in this $k$ region. So, we have determined the amplitude and phase functions in an indirect way. We have first used the amplitude and phase-shift functions calculated by the FEFF code.[11] We have fitted the experimental MA spectrum with these functions. The result is shown on Fig. 4(a). It leads to a wrong determination of the distances: $R_1=2.89$ and $R_2=3.17$ Å. This must be due to a slight inaccuracy of the FEFF code for the calculation of the phase shifts. Then, we have modified the phase function by adjusting its slope, to obtain the same fitting curve, but with the real distances. The obtained phase function is compared to the FEFF calculation in Fig. 4(b).

If the $\chi_2$ and $\chi_3$ terms are neglected in the general EXAFS formula (1), the other spectra have to be fitted using these amplitude and phase functions. For these fits, the numbers of neighbors ($N^*$) have been fixed to their calculated values (see Table I). The free parameters are the two distances $R_1$ and $R_2$ and the associated Debye-Waller factors. Two results are shown on Fig. 5 for two incident angles $\alpha=0°$ and 80°. For the normal incidence ($\alpha=0°$) spectrum (where we have the higher contribution of the in-plane NN) we obtain $R_1=3.00$ instead of 2.97 Å, and for the grazing incidence spectrum ($\alpha=80°$) (where we have the higher contribution of the out-of-plane NN's) we obtain $R_2=3.36$ instead of 3.254 Å. In Table II, we give the results of the fits for all the incident angles ($\alpha$): bond lengths appear to be very different depending on $\alpha$. The bond lengths variation reaches 0.06 Å for the first distance and 0.13 Å for the second one. This error is very important and shows that the assumption of $c=0$ for anisotropic systems is not accurate. The quality of the fits is correct. Then, if the structure of the sample is unknown, and $\chi_2$ and $\chi_3$ are supposed to be neg-

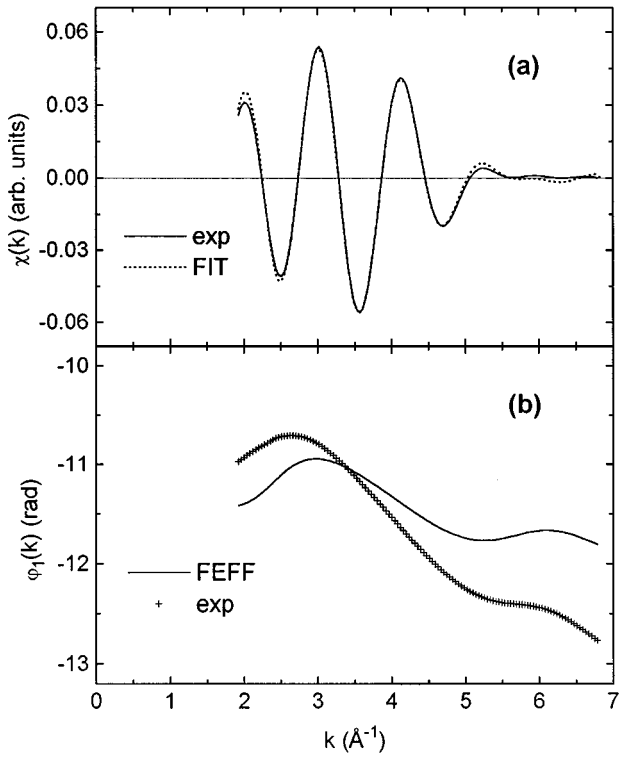


FIG. 4. (a) Fit (dotted line) of the experimental first-nearest-neighbors shell contribution to the EXAFS signal (solid line) recorded at the magic angle on Cd(0001). This contribution is extracted from the total signal by backtransforming in $k$ space the first peak of the Fourier transform of the spectrum (between $R=1.96$ and $R=3.80$ Å). (b) Total phase shift functions (i) calculated with the FEFF code (solid line), and (ii) modified to obtain the real $R_1$ and $R_2$ distances in the fit (crosses).

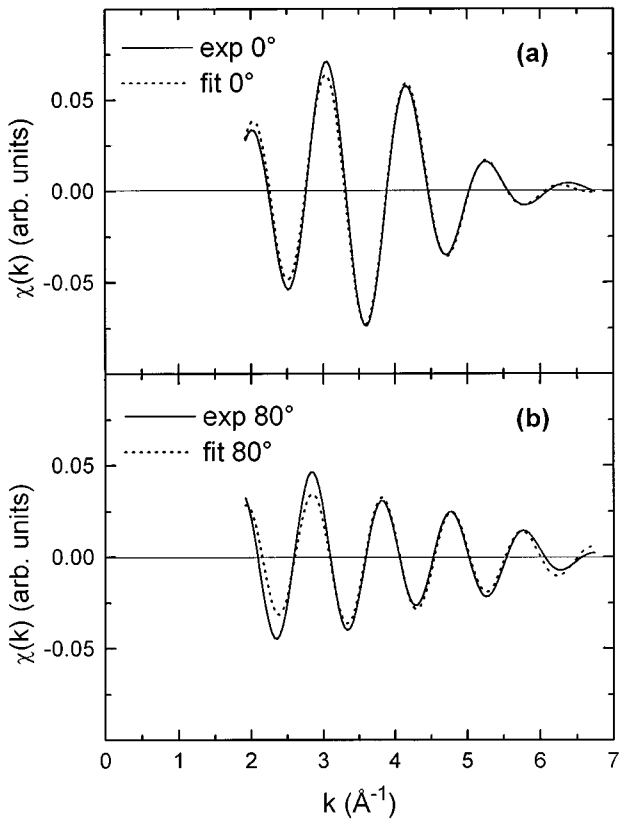


FIG. 5. Fits (dotted lines) of the experimental first-nearest-neighbors shell contribution to the EXAFS signal (solid lines) recorded at $\alpha=0°$ (a) and $\alpha=80°$ (b) on Cd(0001). These fits are done neglecting the $\chi_2$ and $\chi_3$ terms.

ligible, the fits will not show evidence of a problem, but the structural determination will be incorrect.

TABLE II. Structural parameters obtained by fitting the experimental first-nearest-neighbors shell contribution to the EXAFS signal. In these fits, the $\chi_2$ and $\chi_3$ terms are neglected.

| $\alpha(°)$ | 0 | 15 | 30 | MA | 45 | 60 | 70 | 80 |
|---|---|---|---|---|---|---|---|---|
| $R_1$ (Å) | 3.00 | 3.00 | 2.97 | 2.97 | 2.96 | 2.95 | 2.94 | 2.95 |
| $R_2$ (Å) | 3.23 | 3.265 | 3.25 | 3.25 | 3.27 | 3.30 | 3.32 | 3.36 |

## V. DIRECT EVIDENCE OF $c\neq 0$ AND $\Delta\varphi\neq 0$

To know if the error in the distance determination shown above is due to the $\chi_2$ term or to a bad determination of amplitude and phase functions, we have used another analysis technique for which the knowledge of backscattering amplitude and phase shifts is not needed.[12,13] The formula of EXAFS [Eq. (3)] can be rewritten as

$$\chi(k)=\frac{A'(k)}{kR^2}|\widetilde{P}(k)|\sin\{\arg[\widetilde{P}(k)]\}$$

with several approximations: we assume that the Debye-Waller term and the $1/R^2$ terms can be taken out of the sum (this approximation is accurate if $[(\Delta R/R_1)=(R_2-R_1)/R_1$ is small] and that the plane-wave approximation (same phase functions for the two shells) is correct. For the case of cadmium, considering formula (3) we have

$$\widetilde{P}(k)=N_1^* e^{j2kR_1}e^{j\varphi_1}+N_2^* e^{j2kR_2}e^{j\varphi_1}+cN_1^{**}e^{j2kR_1}e^{j\varphi_1}e^{j\Delta\varphi}+cN_2^{**}e^{j2kR_2}e^{j\varphi_1}e^{j\Delta\varphi}.$$

With the approximation $(\Delta R/R_1)\ll 1$, we have $N_1^{**}=-N_2^{**}$, and $N_1^*+N_2^*=12$ (see Sec. III), then

$$\arg[\widetilde{P}(k)]=k(R_1+R_2)+\varphi_1+\arctan\left(\frac{(N_2^*-N_1^*)\sin(k\Delta R)-cN_1^{**}[\sin(k\Delta R-\Delta\varphi)+\sin(k\Delta R+\Delta\varphi)]}{(N_1^*+N_2^*)\cos(k\Delta R)+cN_1^{**}[\cos(k\Delta R-\Delta\varphi)-\cos(k\Delta R+\Delta\varphi)]}\right).$$

$\arg[\widetilde{P}(k)]$ is the total phase of the NN EXAFS signal. Due to the interference between the different shells, kinks occur in $\arg[\widetilde{P}(k)]$ when the denominator of the function in arctan is equal to zero. The corresponding value of $k$, $k_b$, is the position of the beating. That occurs when

$$c\sin\Delta\varphi\tan(k_b\Delta R)=-\frac{N_1^*+N_2^*}{2N_1^{**}}\cong\frac{2}{3\cos^2\alpha-2}. \quad (4)$$

If $c=0$ or $\Delta\varphi=0$, the condition of the beating should be $\cos(k_b\Delta R)=0$. Therefore, if the position of the beating is depending on $\alpha$, it is a proof that $c=0$ and $\Delta\varphi=0$.

In practice, the kink position is located by taking the derivative of the NN shell phase with respect to $k$. Figure 6 shows the results for the derivative of the phase as function of $k$ for different values of $\alpha$. One can see that the position of the maximum of the derivative is depending on $\alpha$: the beating node is at 5.80 Å$^{-1}$ for $\alpha=30°$, 5.21 Å$^{-1}$ for $\alpha=45°$, and 4.86 Å$^{-1}$ for $\alpha=60°$. For the other angles the position of the beating is more difficult to determine because of the smaller bump, which can be due to the values of $(N_1^*/N_2^*)$ far from 1. This variation of the position of the beating with $\alpha$ is coherent with the results of the above fit of the NN shell: we found that assuming $c=0$ was leading to a $\Delta R$ value increasing with $\alpha$ (see Table II). Considering formula (4), the position of the beating in the MA spectra ($k_b=5.59$ Å$^{-1}$) leads to the expected value of $\Delta R=0.28$ Å. Using formula (4), we estimate the value of $c\sin\Delta\varphi$, which induces the measured shift with $\alpha$ of the beating position. We obtain $c\sin\Delta\varphi=-0.4\pm0.1$. Knowing that $|\sin\Delta\varphi|\leqslant 1$, we can say that $c\geqslant 0.4$. It is a value two times larger than the one calculated by Teo and Lee[9] or experimentally determined on a weakly anisotropic system.[6]

The accuracy of the approximations used for the beating analysis is tested on theoretical spectra calculated by FEFF.[11]

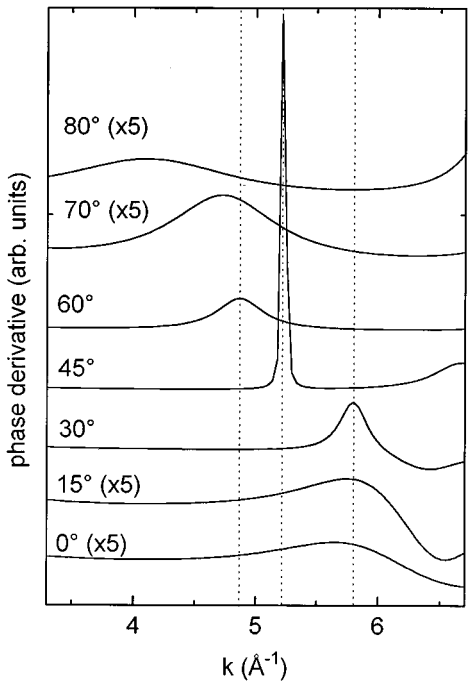


FIG. 6. Derivative of the phase of the experimental first-nearest-neighbors shell contribution to the EXAFS signal recorded for different incident angles of the x rays.

FEFF calculates single and multiple-scattering curved wave EXAFS spectra assuming $c=0$. We have simulated cadmium $L_3$ absorption spectra with $\alpha=0°$, 15°, 45°, 60°, 70°, and 80°. The spectra have been analyzed in the same manner as the experimental ones and we have determined the position of the beating node by looking at the derivative of the phase. The beating node positions are not depending on the $\alpha$ angle. Using formula (4), we obtain $-0.09 \leqslant c \sin\Delta\varphi \leqslant 0.06$. So, this analysis is self-consistent.

Qualitatively, the above beating analysis provides us with the following results: the $\chi_2$ term cannot be neglected and the value of $c$ is at least about 0.4. Due to the approximations we used, the above determination is rough and qualitative. In the next section, we proposed a quantitative determination of the $\chi_2$ term.

## VI. ESTIMATION OF THE $\chi_2$ TERM

Let us try now to evaluate more precisely the $\chi_2$ term. At the first order in $c$, we can rewrite Eq. (3):

$$\chi(k)=\chi_1(k)+\chi_2(k)=\chi_1(k)+N_1^{**}\chi_2'(k).$$

Then

$$\chi_2'(k)=\frac{\chi(k)-\chi_1(k)}{N_1^{**}} \tag{5}$$

and, from formula (3),

$$\chi_2'(k)=cA'(k)\left(\frac{1}{kR_1^2}\sin(2kR_1+\varphi_1+\Delta\varphi)-\frac{h^2-2}{kR_2^2}\sin(2kR_2+\varphi_1+\Delta\varphi)\right).$$

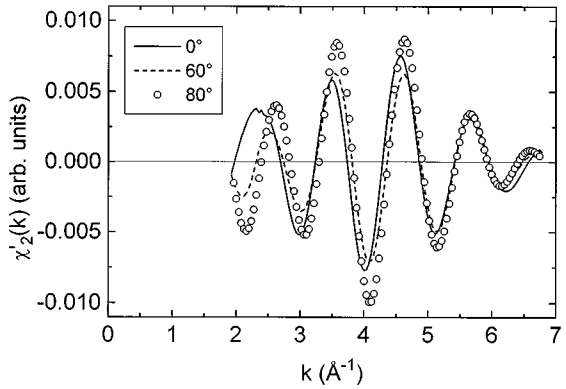


FIG. 7. $\chi_2'(k)$ term extracted from the experimental spectra recorded at $\alpha=0°$ (solid-line), $\alpha=60°$ (dashed line), and $\alpha=80°$ (open circles).

$\chi_1(k)$ is calculated with the functions $A'(k)$ and $\varphi_1(k)$ extracted from the MA spectrum. If the above formula is correct $\chi_2'(k)$ should be independent on $\alpha$. So, it is extracted from the experimental data for each angle, using formula (5). The results are shown in Fig. 7. We find similar curves: they are in phase except at low $k$ and the amplitude is slightly dependent on the incident angle. Considering the values of $N_1^{**}$ (see Table I) the best determination of $\chi_2'$ is made at 80°. Then, to test the validity of the $\chi_2'$ determination, we have compared for each angle the experimental spectra with the sum of $\chi_1(k)$ (calculated with the MA parameters) and $\chi_2(k)$ (determined at 80°). On Fig. 8, we have plotted the experimental spectra, the $\chi_1$ term and the sum $\chi_1+N_1^{**}\chi_2'$. We see that, for all cases, the introduction of the $\chi_2$ term improves considerably the simulation: we obtain a better agreement between experiment and simulations both for amplitude and phase. We see that if at 30° the effect of the $\chi_2$ term is small (near the magic angle, the correction is small) this effect is large for the other angles. That explains the big errors which are made by neglecting the $\chi_2$ term in the fits.

We can now estimate the $c$ and $\Delta\varphi$ values. We can extract them from the $\chi_2'$ spectra. The expression of $\chi_2'$ is

$$\chi_2'=cA'(k)\left(\frac{1}{kR_1^2}\sin(2kR_1+\varphi_1+\Delta\varphi)-\frac{h^2-2}{kR_2^2}\sin(2kR_2+\varphi_1+\Delta\varphi)\right).$$

If we compare this function with

$$\chi_1'=A'(k)\left(\frac{1}{kR_1^2}\sin(2kR_1+\varphi_1)-\frac{h^2-2}{kR_2^2}\sin(2kR_2+\varphi_1)\right),$$

we can determine $c$ and $\Delta\varphi$:

$$c=\frac{\mathrm{amp}(\chi_2')}{\mathrm{amp}(\chi_1')} \quad \text{and} \quad \Delta\varphi=\mathrm{phase}(\chi_2')-\mathrm{phase}(\chi_1').$$

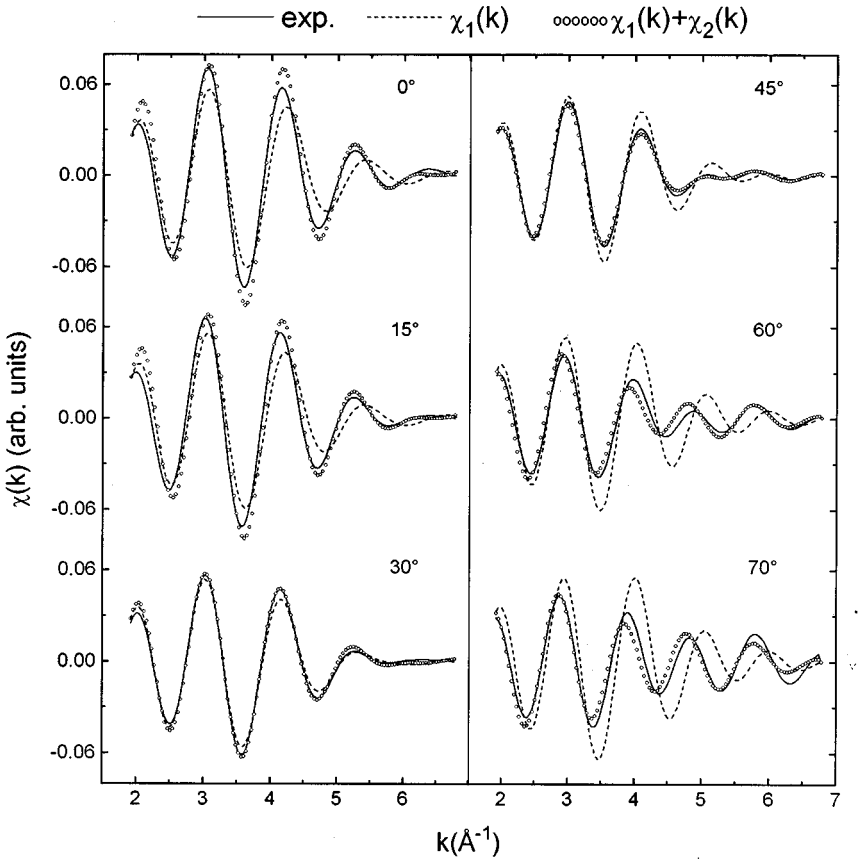


FIG. 8. Comparison between the experimental first-nearest-neighbors shell contribution to the EXAFS signal (solid line), $\chi_1(k)$ calculation (dashed line), and $\chi_1(k)+\chi_2(k)$ calculation (open circles), for different incident angles of the x rays.

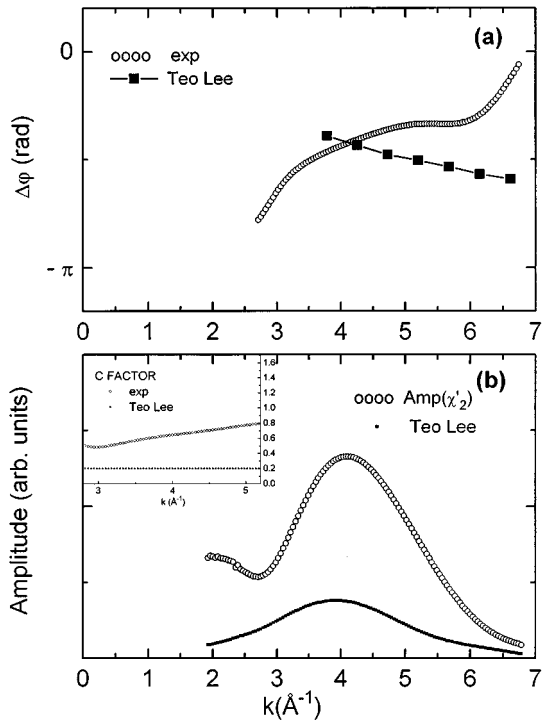


FIG. 9. (a) $\Delta\varphi$, (b) amplitude of the $\chi'_2(k)$ term and value of $c$ determined from the experimental spectra (open circles) and calculated by Teo and Lee[9] (closed squares).

These functions are plotted in Fig. 9. They are compared to the calculation of Teo and Lee[9] [Figs. 9(a) and 9(b)]. The value of $\Delta\varphi$ is about $-(\pi/2)$, as was predicted by the theory, but the amplitude ratio is much higher than the predicted one. The value of the $\chi'_2$ amplitude is particularly important in a $k$ window between 3 and 5 Å$^{-1}$. In this region, the value of $c$ is between 0.4 and 0.75. This result is in agreement with our previous determination using the position of the beating node, but it is different from the theoretical calculation[9] and the previous experimental determination,[6] which gave $c=0.2$. This discrepancy is more important than the error bar of our experimental determination.

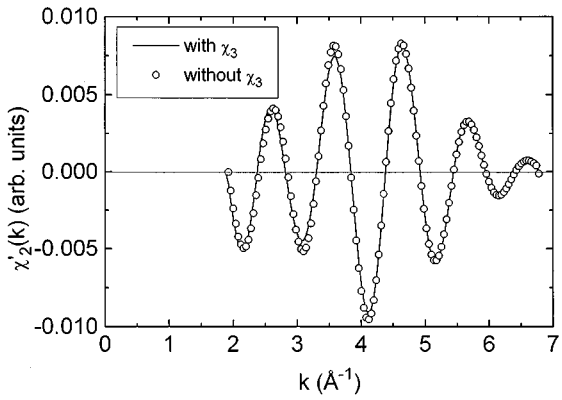


FIG. 10. Calculation of the $\chi'_2(k)$ term (i) taking into account the $\chi_3(k)$ term (solid line), and (ii) without taking into account the $\chi_3(k)$ term (open circles).

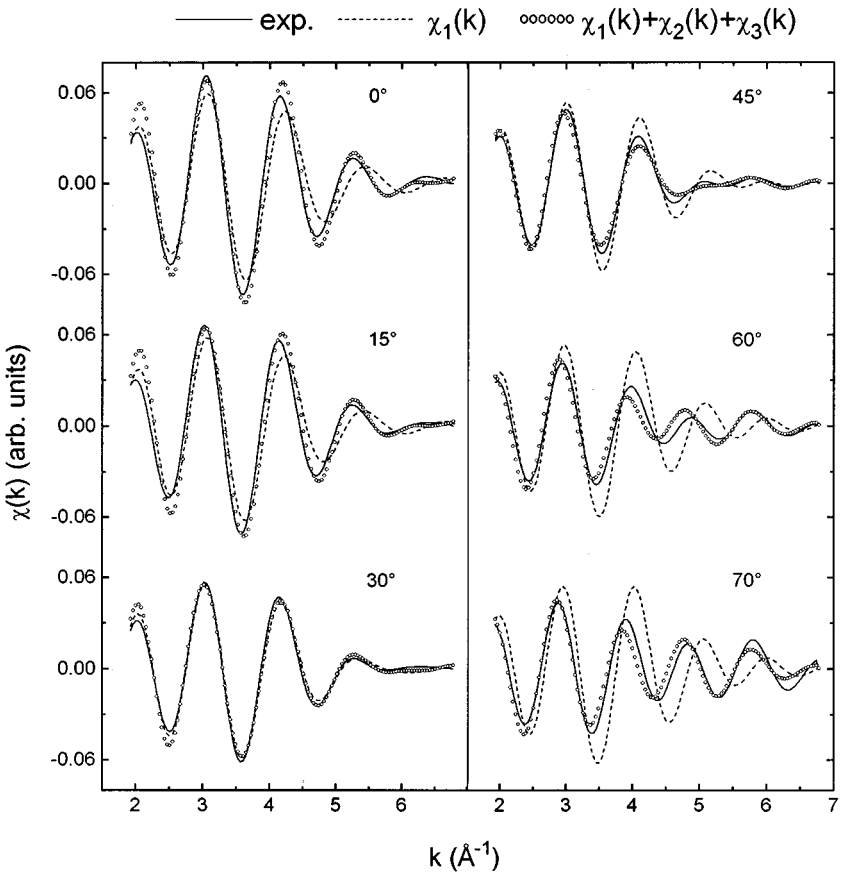


FIG. 11. Comparison between the experimental first-nearest-neighbors shell contribution to the EXAFS signal (solid line), $\chi_1(k)$ calculation (dashed line), and $\chi_1(k)+\chi_2(k)+\chi_3(k)$ calculation (open circles), for different incident angles of the x rays.

### VII. THE $\chi_3$ TERM EFFECT

If $c \approx 0.5$, one can argue now that the first approximation we have done (i.e., $\frac{1}{2}c^2 \ll 1$) is not accurate. We have to test the consistency of our study. The knowledge of $c$ and $\Delta\varphi$ allows us to calculate the term $\chi_3$ and to introduce it in formula (3):

$$\chi_3 = \tfrac{1}{2}\, c^2 A'(k)\left(\frac{6}{kR_1^2}\sin(2kR_1+\varphi_1+2\Delta\varphi)+\frac{6}{kR_2^2}\sin(2kR_2 + \varphi_1+2\Delta\varphi)\right).$$

We have obtained a value of $\Delta\varphi$ around $-(\pi/2)$. Then the $\chi_3$ term is approximately in phase opposition with the $\chi_1$ term. Its effect is to apparently reduce the number of neighbors ($N^*$) by a value of 0.75 (taking $c=0.5$), not depending on the value of $\alpha$. Therefore, it induces an increase of the relative weight of the neighbors that give the predominant contribution to the signal (in-plane NN for $\alpha=0°$, out-of-plane NN for $\alpha=80°$) by about 4%. We can say that the effect should be small.

To check that, we have calculated $\chi_3$ using $c$ and $\Delta\varphi$ determined with the assumption that $c$ is small. This $\chi_3$ term is subtracted from the experimental MA spectrum. We make then a new fit of the resulting spectrum as in Sec. IV. The new amplitude and phase functions are very similar to the previous ones. This result validates the approximation made on isotropic systems: neglecting $\chi_3$ in a situation where $\chi_2$ is zero (isotropic systems or magic angle for an anisotropic system) yields to an error in the bond length determination of 0.01 Å , and less than 10% for the number of neighbors.

The new amplitude and phase functions are used to calculate a new $\chi_1$ and a new

$$\chi_2'(k) = \frac{\chi(k)-\chi_1(k)-\chi_3(k)}{N_1^{**}}.$$

This function is plotted with the old one in Fig. 10. The difference is very small and leads to the same value of $c$ and $\Delta\varphi$. At last, we compare the experimental spectra with the sum: $\chi_1+\chi_2+\chi_3$ (Fig. 11). The agreement is as good as the previous one. Then we conclude that the $\chi_3$ term can be neglected in the evaluation of the relative importance of the $\chi_2$ and $\chi_1$ terms. The rough evaluation of $\chi_2$ done with the angular dependence of the position of the beating node was not so bad: it gave $c\sin\Delta\varphi \approx -0.4$. We finally obtain $\sin\Delta\varphi \approx -1$ and $c \approx 0.5$. So, the test of the beating position is a good one to estimate if $\chi_2$ has to be considered and to determine which is its relative weight.

### VIII. CONCLUSION

In this study, we have evaluated the importance of the $p$ and $s$ transitions for the $L_3$-edge absorption spectrum in an anisotropic system. We have shown that the crossed term that coupled final states of $s$ and $d$ symmetries cannot be neglected: it represents an important contribution to the measured signal. Since this term has an angular dependence different from the main one, neglecting it leads, in our case, to

errors in bond-length determination as high as 0.1 Å.

In cadmium, the effect of this crossed term, $\chi_2$, is important because the structure is strongly anisotropic: for example, at 80° $(N_1^{**}/N_1^{*})=1.82$ and $(N_1^{**}/N_2^{*})=0.62$. The study of this kind of structure at $L_{2,3}$ absorption edges is important for surface science: surfaces and thin films are also very anisotropic systems and one can expect here also a high contribution of the $\chi_2$ term. The tests done on quite isotropic systems are less meaningful, since the main correcting term is *a priori* small. Moreover, we have obtained a very good sensitivity to the anisotropy by measuring the experimental XAFS spectra in a large angular domain: we have varied the incident angle of the x rays from 0° to 80°.

As a conclusion, if one wants to use surface EXAFS at the $L_{2,3}$ edges to extract structural parameters, one has to be very careful with the angular dependence of the signal. It is not possible to extract at the same time structural parameters and the relative weight of the different transition channels $p$ to $s$ and $p$ to $d$. For the near future, an accurate calculation of these two terms is hopefully expected.

## ACKNOWLEDGMENTS

We acknowledge Elisabeth Dartyge and John Rehr for fruitful discussions.

[1] L. I. Johansson and J. Stöhr, Phys. Rev. Lett. **43**, 1882 (1979).
[2] F. Comin, J. E. Rowe, and P. H. Citrin, Phys. Rev. Lett. **51**, 2402 (1983).
[3] L. Tröger, T. Yokoyama, D. Arvanitis, T. Lederer, M. Tischer, and K. Baberschke, Phys. Rev. B **49**, 888 (1994).
[4] P. Roubin, D. Chandesris, G. Rossi, J. Lecante, M. C. Desjonquères, and G. Treglia, Phys. Rev. Lett. **56**, 1272 (1986).
[5] E. A. Stern, Phys. Rev. B **10**, 3027 (1974).
[6] S. M. Heald and E. A. Stern, Phys. Rev. B **16**, 5549 (1977).
[7] P. H. Citrin, Phys. Rev. B **31**, 700 (1985).
[8] C. Brouder, J. Phys. Condens. Matter **2**, 701 (1990).
[9] B. K. Teo and P. A. Lee, J. Am. Chem. Soc. **101**, 2815 (1979).
[10] J. Stöhr and R. Jaeger, Phys. Rev. B **27**, 5146 (1983).
[11] J. J. Rehr, J. Mustre de Leon, S. I. Zabinsky, and R. C. Albers, J. Am. Chem. Soc. **113**, 5135 (1991); J. J. Rehr, S. I. Zabinsky, and R. C. Albers, Phys. Rev. Lett. **69**, 3397 (1992).
[12] G. Martens, P. Rabe, N. Schwentner, and A. Werner, Phys. Rev. Lett. **39**, 1411 (1977).
[13] D. T. Jiang, E. D. Crozier, and B. Heinrich, Phys. Rev. B **44**, 6401 (1991).